

Characterization of Transient-Large-Amplitude Geomagnetic Perturbation Events

Brett A. McCuen¹, Mark B. Moldwin¹, Mark Engebretson²

¹University of Michigan, Ann Arbor, Michigan
²Augsburg University, Minneapolis, Minnesota

Key Points:

- Short-timescale (< 60 s) geomagnetic perturbation events found at 6 high-latitude MACCS stations throughout 2015 are characterized
- Transient-large-amplitude magnetic perturbation events often occur in close relation to or within larger geomagnetic disturbances
- TLA events suggest small-scale ionospheric currents but exact source mechanisms are still unclear

Corresponding author: Brett A. McCuen, bmccuen@umich.edu

This is the author manuscript accepted for publication and has undergone full peer review but has not been through the copyediting, typesetting, pagination and proofreading process, which may lead to differences between this version and the [Version of Record](#). Please cite this article as [doi: 10.1029/2021GL094076](https://doi.org/10.1029/2021GL094076).

This article is protected by copyright. All rights reserved.

Abstract

We present a characterization of transient-large-amplitude (TLA) geomagnetic disturbances that are relevant to geomagnetically induced currents (GIC). TLA events are defined as one or more short-timescale (< 60 seconds) dB/dt signature with magnitude ≥ 6 nT/s. The TLA events occurred at six stations of the Magnetometer Array for Cusp and Cleft Studies throughout 2015. A semi-automated dB/dt search algorithm was developed to identify 38 TLA events in the ground magnetometer data. While TLA dB/dts do not drive GICs directly, we show that second-timescale dB/dts often occur in relation to or within larger impulsive geomagnetic disturbances. Sudden commencements are not the main driver, rather the events are more likely to occur 30 minutes after a substorm onset or within a nighttime magnetic perturbation event. The characteristics of TLA events suggest localized ionospheric source currents that may play a key role in generating some extreme geomagnetic impulses that can lead to GICs.

Plain Language Summary

Severe space weather events like geomagnetic storms and substorms cause geomagnetically induced currents (GIC) in electrically conducting material on Earth that are capable of damaging transformers and causing large-scale power grid failure. GICs are driven by large changes of the surface geomagnetic field, dB/dt , that have timescales of minutes to tens of minutes. Magnetic field variations with shorter-timescales (< 60 s) are not capable of driving large GICs directly, but we show here that they often occur in relation to or within larger storms, substorms and magnetic pulsation events that are capable of driving substantial GICs. In this study, we characterize these transient-large-amplitude (TLA) geomagnetic perturbation events and examine them in the context of other space weather events.

1 Introduction

Space weather events occur due to the interaction of active solar wind with near-Earth space, activating magnetohydrodynamic (MHD) and electromagnetic transfer processes that propagate throughout the magnetosphere-ionosphere (M-I) system down to the surface of Earth. Perhaps the most critical concern regarding space weather is the threat of large geomagnetically induced currents (GIC) to technological infrastructure on Earth. Flowing through man-made conductors on Earth like railways, pipelines and power grids, GICs can be large enough to cause damage to transformers resulting in major power outages and costly equipment damage (Boteler et al., 1998; Pulkkinen et al., 2017). GICs are the result of a horizontal surface electric field \mathbf{E} induced in Earth's surface that is driven by large changes of the surface magnetic field, dB/dt , via Faraday's law of induction. Hazardous GICs associated with large, rapid magnetic disturbances often result from the most disruptive geomagnetic storms and auroral substorms. Therefore, significant efforts of the geophysical community are aimed at developing global MHD models of geomagnetic storm and substorm activity and incorporating the magnetotelluric response of the Earth to compute GICs (Pulkkinen et al., 2015; Zhang et al., 2012). However, beyond the largest space weather events, several studies suggest that there are more rapid, small-scale and localized processes involved in generating some extreme GICs (Dimmock et al., 2020; Engebretson et al., 2019a, 2021; Ngwira et al., 2015, 2018; Opgenoorth et al., 2020).

Impulsive geomagnetic disturbances as a source of GICs were first reported by Kappenman (2005). More recently, Belakhovsky et al. (2019) presented case studies of impulsive magnetic events such as sudden commencements (SC), dayside traveling convection vortices (TCV), nightside magnetic perturbation events (MPE) and irregular Pi3 pulsations that can all induce substantial GIC. These impulsive disturbances are in the lower range of the ultra-low frequency (ULF) band from 1-22 mHz with periods of 1-10 minutes. Shorter-timescale (< 1 minute) perturbations of the geomagnetic field are much less effective at generating GICs due to their frequency content. Because of the skin depth effect in a conducting medium, lower frequencies penetrate deeper into the Earth, increasing the size of the induction loop and subsequent induced currents while higher frequencies

can only penetrate to shallow depths, resulting in much smaller induction loops that are incapable of driving GICs (Oyedokun et al., 2020). While extreme dB/dts with second timescales do not cause GICs on Earth directly, we show here that they often occur in close relation to or within larger impulsive disturbances that *are* capable of generating GICs. These rapid magnetic perturbations in the Pi 1-2 frequency range may be ground manifestations of small-scale ionospheric current systems that play an important role in driving localized, but considerable GICs.

In this study, we present occurrences of transient-large-amplitude (TLA) dB/dts that occurred at one or more of six stations of the Magnetometer Array for Cusp and Cleft Studies (MACCS) throughout 2015. These perturbations all have amplitudes comparable to geomagnetic disturbances that cause large GICs, but have timescales less than 60 seconds. We investigate them here in an effort to gain insight on the transient structures of the geomagnetic field and small-scale M-I coupling mechanisms relevant to GICs. We have characterized these events based on their frequency of occurrence, spatial and temporal dependence, and association (or lack thereof) to longer impulsive magnetic events, substorms and storms.

2 Data Set and Identification Technique

The magnetometer data used in this study are from six ground stations of the MACCS array. The stations are located in north-east Nunavut, Canada (geographic and corrected geomagnetic (CGM) coordinates are listed in Supporting Information Table S1, the stations are shown with lines of CGM latitude in the map of Supporting Information Figure S1.) This paper refers to station locations in CGM coordinates that were calculated for the year of 2015 with the IGRF transformation tool of the World Data Center (WDC) for Geomagnetism, Kyoto. The MACCS magnetometers collect 8 samples per second in three axes, then average and record the data at two samples per second (Hughes & Engebretson, 1997). The half-second sampling rate and high sensitivity (0.01 nT resolution) of the MACCS magnetometers is sufficient to detect shorter period Pi 1 and 2 pulsations. The geomagnetic variations measured by the magnetometers are in local geomagnetic coordinates: X (north-south), Y (east-west) and Z (vertical).

A semi-automated algorithm was developed to identify dB/dt signatures in magnetometer data with user-specified duration and magnitude. After initial data processing to remove instrument artifacts and smooth the data with a sliding average (if desired and with user-specified window length), the algorithm is essentially a series of filters. First the algorithm calculates the slope between each and every data point and determines the sign of the slope (assigns a 1 if positive slope, -1 if negative slope). If the sign of the slope changes for at least 1-second (two data points), the data point at which this change occurs (i.e. local minima or maxima) is flagged. Then the last filter recalculates the new dB/dt between each local maxima and minima and returns the information of the signature if it meets the conditions of the defined thresholds for dB/dt and Δt . The final product returned from the algorithm is a seven column matrix, each row represents an individual event and provides the start and end time of the event, start and end B value, the time elapsed of the event: dt , the change in magnetic field amplitude: dB , and the total perturbation: dB/dt .

We used this algorithm to identify dB/dt signatures with amplitude 6 nT/s or higher and duration less than 60 seconds. The dB/dt threshold is comparable to the surface magnetic field perturbations (~ 8 nT/s) that caused the HydroQuebec power grid to fail during the geomagnetic storm of March 1989 (Kappenman, 2006). We characterize a transient-large-amplitude (TLA) event as one or more of these dB/dt signatures if they occur within 1-hour of another (regardless of the axis measured in and the station measured at). Because of the timescale and magnitude of the dB/dts sought, many of these signatures are similar in nature to magnetometer noise caused either by instrumental artifacts or magnetic deviation due to interference by ferromagnetic materials in the vicinity of the magnetometer (Nguyen et al., 2020). Therefore, each event returned from the routine was visually inspected to confirm that it appeared to be of physical nature or remove it if it was a result of noise. In our manual inspection process, we found that the events resulting from magnetometer noise have several characteristics that make them possible to auto-

matically detect. Our future work will incorporate a machine learning noise identification method that will help to fully automate the dB/dt search algorithm and contribute to magnetic noise cleaning approaches for other magnetometer arrays.

After the filtering process, a total of 178 transient-large-amplitude dB/dt signatures were identified. The majority of these signatures (61%) were measured in the x-component (north-south), 30% in the y-component (east-west) and 9% in the z-component (vertical). Finally, grouping the dB/dts if they occurred within 1 hour of another signature resulted in a total of 38 TLA dB/dt events. While the primary temporal periods of interest in this study are 1-60 seconds, we also ran the algorithm with the upper limit for the duration of events extended to 5 minutes in order to compare to the 5-10 minute lasting MPEs studied in Engebretson et al. (2019a). Note that we used cleaned, full resolution half-second magnetic field data in this study and GIC measurement often involves averaging magnetometer data over 1 minute (Ngwira et al., 2008; Pulkkinen et al., 2006). Because our identification method relies on changes of the magnetic field lasting at least 1 second, some larger and more extended dB/dts are undetected by our algorithm due to more rapid changes of the slope within.

Our analysis of TLA event dependence on space weather events relies on several databases. The SuperMAG database (Gjerloev, 2012) Ring Current (SMR) index (Newell & Gjerloev, 2012) was used to determine geomagnetic storm activity and the SuperMAG Electrojet indices (SME) (Newell & Gjerloev, 2011) were used to examine auroral sub-storm activity during the events (supermag.jhuapl.edu/indices/). The association of TLA events with SCs was determined with the International Service of Geomagnetic Indices Sudden Commencement event list (isgi.unistra.fr/events_sc.php).

3 Occurrence of Transient-Large-Amplitude (TLA) dB/dt Events

We identified 38 TLA events consisting of one or more dB/dt signatures with magnitude 6 nT/s or higher and duration less than 60 seconds. Over half of the events (55%) have multiple dB/dt signatures. Seven of the 38 TLA events exhibit dB/dts that last less than 10 seconds; in six of these cases the < 10 s signatures precede a larger-amplitude, longer-timescale dB/dt . Figure 1 shows three panels with examples of distinct TLA events identified at the MACCS stations in 2015. The hollow circles in all three panels of Figure 1 mark the start of each dB/dt within the TLA event and the solid dots mark the end of each dB/dt . Note that axes in all plots of Figure 1 have been adjusted by subtracting the mean $B_{x,y,z}$ value from the interval, so the magnitude of the rate of change of the magnetic field is still to scale.

We expected to find many events occurring due to SCs as they have been considered the primary driver for the most rapid GICs (Kataoka & Ngwira, 2016). SCs are classified as storm-sudden-commencement (SSC) if followed by the main phase of a geomagnetic storm and as sudden impulse (SI) if not (Curto et al., 2007). We found only one SSC-related event, shown in Figure 1a. This is the only SC-related event despite five recorded SSCs and two SIs that occurred in 2015 when the MACCS stations were located on the dayside. This TLA event started on 22 June 2015 at 18:33:22 UT (12:41:22 MLT, at RBY), just seconds after a large CME reached Earth causing an SSC at 18:33 UT. The largest dB/dt signature of the entire data set occurred in this event at RBY in the y-component, lasting 9.5 seconds with a magnitude of -33.49 nT/s. The dB/dts measured in the y- and z-components at PGG and CDR all last 10.5 seconds or less, with the shortest event in the y-component at CDR with a magnitude of 13.3 nT/s and lasting just 5 seconds.

Shown in Figure 1b is an event that occurred on 11 November 2015 beginning at 01:12:20 UT (21:22:36 MLT of 10 November 2015). This event consists of 34 dB/dts measured at all but the NAN station. Of these 34 dB/dts , six have magnitude greater than 10 nT/s and five have duration < 10 seconds. One of the largest dB/dts (16.2 nT/s) was measured at PGG at 1:13:21 UT in the y-component and lasted only 1 second. The TLA dB/dts occur at each station within a ~ 6 minute interval and occur within a nighttime MPE event (Engebretson et al., 2019b). The TLA and MPE event occur within a longer

Figure 1. (a): A TLA event that occurred on 22 June 2015. (b): An event that occurred on 11 November 2015. (c) An event that occurred on 9 October 2015. All three panels show the x, y and z components of the surface magnetic field from top to bottom, respectively. Hollow circles mark the start of a dB/dt signature and solid dots mark the end.

Figure 2. Maximum dB/dt as a function of magnetic local time (MLT) of each TLA event found in 2015. The bars extended from some squares signifies the duration of an event with multiple dB/dts . The opacity of squares is based on the temporal proximity after the nearest substorm onset. The inner red squares signify unrelated events that occurred more than 30 minutes from substorm onset and in the absence of a storm or nighttime MPE.

period of disturbance that lasted ~ 1 hour; they are not associated with a geomagnetic storm, although a substorm onset occurred at 01:07 UT, about 5 minutes prior to the start of the event. The events were preceded by a steady magnetic field for at least an hour prior to the start of the disturbance around 00:40 UT.

Finally, Figure 1c shows a TLA event on 9 October 2015 starting at 04:26:06 UT at the CDR station (23:31:06 MLT of 8 October 2015) where B_x decreases by 135.9 nT in 21 seconds ($dB_x/dt = -6.46$ nT/s). Then about 14 minutes later, two similar signatures occurred at GJO: a dB_x/dt of -6.87 nT/s at 04:49:37 UT and a dB_y/dt of -6.52 nT/s at 04:41:05 UT. Note, however, that the dB_x/dt at GJO actually lasted 80 seconds, this is one of the signatures identified when extending the upper threshold for the duration of the sample in the search algorithm to 5 minutes rather than 60 seconds. This TLA event occurred on the second day of recovery from a moderate geomagnetic storm and there were marked substorm onsets occurring at 04:13 UT and 4:34 UT. A nighttime MPE was identified at RBY at 04:37 UT in the interval between these two TLA events at CDR and GJO but no TLA signatures were measured within the MPE at RBY (note that the GJO station was not used in the statistical study of Engebretson et al., 2019a).

4 Spatial and Temporal Characteristics and Space Weather Dependence

There are ten TLA events that consist of at least one dB/dt signature with magnitude exceeding 10 nT/s and half of these occurred within an event that has at least one other $|dB/dt| \geq 10$ nT/s. The ten largest events were measured primarily between 73° and 76° CGM latitude at the PGG and CDR stations: PGG and CDR not only recorded the majority of the largest events but a substantial fraction (52.6% and 44.7%, respectively) of events in general. The GJO (76.86°) station recorded eight events and RBY (75.62°) and IGL (78.63°) recorded four events each. The southern-most station, NAN (65.67°), recorded just two events that were not recorded at any other station. In fact, 74% of the events were measured locally at only one station (the average, absolute distance from one station to the nearest station is ~ 580 km. Note this average excludes NAN as it is the lowest latitude station with only two locally recorded events). Of the other 26% of events measured at more than one station, 4 were recorded relatively simultaneously (as shown in Figures 1a and 1b) while 6 other events had dB/dts at more than one station delayed by at least 2 minutes (and at most 14 minutes, shown in Figure 1c).

TLA events occurred substantially more often in the Fall-Winter months with 57.9% of events occurring in October through December. To illustrate the occurrence of TLA events as a function of magnetic local time as well as the association to geomagnetic

Figure 3. Venn diagram of number of TLA events related to geomagnetic storms (with cells specified for storm phases), substorms, and nighttime MPEs, as well as the distinct unrelated events.

storms and substorms, Figure 2 shows the maximum dB/dt of each TLA event throughout 2015 as a function of MLT. The events that occurred between 18-6 MLT are plotted as squares with opacity according to temporal proximity of prior substorm onset: the black squares signify that the event started within 15 minutes after the nearest substorm onset and during nighttime hours of 18-6 MLT, the grey squares are events that occurred 15-30 minutes after substorm onset and the white squares occurred more than 30 minutes after the nearest substorm onset (daytime events were automatically marked as white squares). These onset delays were determined with the SuperMAG Newell and Gjerloev (2011) Substorm Event List (supermag.jhuapl.edu/substorms/). The bars extending from some of the squares in Figure 2 signify the full duration of the event if it consisted of multiple dB/dts , showing at what point throughout the event that the maximum dB/dt occurred. Only three events occurred in the commencement or main phase of a geomagnetic storm, these are labeled in Figure 2. There are also five events that occurred on the first day of recovery from a geomagnetic storm and four events that occurred on the second day of recovery.

Figure 2 shows that a vast majority (92.1%) of events occurred at nighttime between 18-6 MLT with peak number of events (71.1%) in the pre-midnight sector from 18-24 MLT. A large number of the events (73.7%) occurred within 30 minutes of substorm onset, but it is clear from Figure 2 that not all of the nighttime events show this association to substorm onsets (see white squares occurring at nighttime). While there is a strong association of TLA events to substorm onsets, 26.3% of events occurred more than 30 minutes after a substorm onset, with a small subset of events (10.5%) that occurred more than 2 hours after substorm onset. Figure 2 also shows that the ten largest TLA events (≥ 10 nT/s) were more likely to occur between 18-24 MLT and within 30 minutes of a substorm onset, but they did not always occur within 30 minutes of substorm onset.

Comparison to the nighttime MPE events of Engebretson et al. (2019a) found that 73.7% of TLA events either preceded an MPE at one of the six stations within 30 minutes or occurred within the longer-timescale perturbation. Seven of the ten largest > 10 nT/s TLA events were associated to MPEs that also exceeded > 10 nT/s but on 5-10 minute timescales. The MPEs that have TLA dB/dts associated with them comprise less than 5% of the entire set of MPEs identified in 2015, however over half the MPEs that have TLA signatures are among the set of largest MPEs (> 12 nT/s) identified at the MACCS stations during 2015.

Less than 10% of TLA events occurred in the absence of a geomagnetic storm and more than 30 minutes after the nearest substorm onset or nighttime MPE, we classify these as unrelated events (marked in Figure 2 as squares with red centers). While TLA events can occur during quieter geomagnetic conditions, there is a clear tendency for these signatures to appear during conjunctions of space weather events. The Venn diagram of Figure 3 shows the number of TLA events based on their association to other geomagnetic disturbances, showing the overlapping (and lack thereof) of events that can give rise to TLA dB/dts . It was previously noted that the percentage of TLA events related to substorms and nighttime MPEs is the same, but Figure 3 shows that these are not the same set of events. TLA events were most likely to occur in association with a nighttime MPE that commenced within 30 minutes of a substorm onset, however this was not *always* the case. The higher density to the right side of the diagram illustrates that TLA events generally did not occur due to a global geomagnetic event alone; more often there were other, smaller-scale processes involved.

5 Discussion and Conclusions

While TLA dB/dt variations do not drive GICs directly, we show here that they often occur in close relation to or within larger geomagnetic disturbances- like substorms and nighttime MPEs- that can cause GICs. We found that SCs were not the main driver for TLA events; though the large SSC that occurred on 22 June did cause the largest amplitude perturbation, it was the only TLA event associated to an SC despite many occurring over the course of the year. There is a strong association of these events to the onset of substorms as well as an association to nighttime MPEs, but it can be seen in Figure 3 that this is not a perfect correlation (i.e. not all nighttime events are substorm-related). The relationship with substorm onsets appears to be a complicated one, as several events occurred multiple hours after the nearest substorm onset, and many of the substorm-related events also occurred during the main phase or recovery of a geomagnetic storm.

In addition to a clear association to substorm onsets, we found that a majority of our events either preceded or occurred within a nighttime MPE (Engebretson et al., 2019a). These nighttime MPEs are large-amplitude magnetic disturbances with 5-10 minute timescale; the study surveyed MPEs observed in this region of north-east Canada from 2014-2017. Like MPEs, the TLA events identified were often, but not always, associated with substorms on a similar two-thirds basis. Using the spherical elementary current systems (SECS) method (Amm & Viljanen, 1999) and the implementation of this technique by Weygand et al. (2011), a superposed epoch analysis was conducted to investigate the average equivalent ionospheric currents (EIC) and inferred field-aligned currents (FAC) during 21 nighttime MPEs that occurred at CDR from mid-2014 to 2016. Engebretson et al. (2019a) found that the largest of these MPEs were associated to intense westward ionospheric currents 100 km above CDR, coinciding with a region of shear between upward and downward FAC. They also found that the largest horizontal dB/dts occurred slightly south of CDR in a localized region of ~ 275 km. Our TLA events show some similarities to these MPEs: 1) Of all six stations, the PGG and CDR stations measured the greatest number of events as well as the largest-amplitude events ($|dB/dt| \geq 10$ nT/s) and 2) we found only ten events that were measured by more than one station, so the majority of our events ($\sim 73.7\%$) were measured locally at just one station. The localized nature of many TLA disturbances implies that the source currents are localized in the ionosphere (Boteler & Beek, 1999).

More recent research has found extreme local enhancements of the geoelectric field with spatial scale ~ 250 -1600 km (Ngwira et al., 2015); these peak geoelectric fields occur during geomagnetic storms but are highly localized in nature, suggesting smaller-scale, localized ionospheric processes as a source mechanism. Ngwira et al. (2015) suggested localized substorm events as a possible source mechanism for generating localized geoelectric extremes, but the exact processes responsible is yet unknown. The tendency of TLA events to occur within some of the largest MPEs and soon after substorm onset suggests that the TLA dB/dts are signatures of rapid, small-scale ionospheric currents, which could be related to the localized substorm events proposed by Ngwira et al. (2015). However, TLA events also occurred independently of both substorms and MPEs, (as well as geomagnetic storms). Localized instabilities that often occur during substorms but can occur in association with other magnetotail phenomena were suggested by Engebretson et al. (2019a) as a cause for nighttime MPEs. Further investigation of the role of TLA dB/dts within nighttime MPEs may shed light on the fine-scale M-I processes responsible. Our future work will involve an expanded search for TLA events and will include a superposed epoch analysis to investigate the small-scale ionospheric current systems involved in driving TLA events.

In order to better understand our events in the context of these MPEs, we extended the upper threshold of the search algorithm to identify disturbances lasting up to 5 minutes with magnitude > 6 nT/s. We found 25 additional dB/dts that were all related to TLA events that we had already identified. Interestingly, only one signature lasted slightly longer than 2 minutes. We hypothesized that the absence of magnetic perturbations in the 2-5 minute timescale range could be due to algorithm bias. Because the method of the routine searches for changes in the direction of the slope (dB/dt) with the condition that the change last for at least 1 second, and we used raw magnetic field data without any smoothing method, it was possible that the algorithm could be missing collections of

dB/dt signatures lasting 2-5 minutes because there are shorter timescale variations occurring within them that did not meet the threshold of 6 nT/s. To test this theory, we applied a 10-point sliding average filter on the magnetic field data (as was done in Engebretson et al. (2019a)) so that any of these shorter variations would be smoothed over, then ran the search algorithm for disturbances lasting up to 5 minutes again. When the data were smoothed, the algorithm identified all the same events as with raw data and identified 17 new events. With the smoothed data, all the events with signatures lasting > 60 seconds were the same apart from one case where the smoothed data marked the magnetic field response to the SSC at RBY as a disturbance lasting 60.5 seconds rather than 34 seconds. This occurred in many cases where the 10-point smoothing altered the exact moment the signature started or ended (subsequently altering the amplitude characteristics as well). While the smoothing method resulted in many signatures marked as having longer duration, there was still only a small number of dB/dts with > 1 minute timescale (32 as opposed to 25 with raw data) and the longest signature lasted 147 seconds. By comparing our results with smoothed data, we verified the methodology of the algorithm and determined that the absence of large-amplitude (> 6 nT/s) magnetic disturbances with timescale 2.5-5 minutes is not due to algorithm bias. This finding suggests that all longer-timescale magnetic perturbations at these stations consist of more rapid variations lasting less than ~ 2.5 minutes, with a vast majority <60 seconds.

What we learned from the error analysis of this study is that a common smoothing method on the data altered the timing and amplitude of the events (sometimes removing signatures altogether), suggesting that the short-timescale nature of the geomagnetic field could often be altered with common data processing methods or missed altogether with 1-minute or even 10-second averaged magnetic field data. While TLA events show a clear association with substorm activity as well as many shared characteristics with nighttime MPEs, they are not consistently related to these space weather events. We found a small subset of TLA events that are unrelated to geomagnetic storms, auroral substorms and nighttime MPEs. TLA events show a localized behavior with a weak association to geomagnetic storms, suggesting that there are other physical mechanisms, even beyond substorms, for localized extreme enhancements in the geomagnetic field. Finally, we show that these signatures can have amplitude of the same order as events that can drive GICs and they often occur in close temporal relation to or within these longer-timescale disturbances. Our future work will include a statistical analysis on an expanded set of TLA events to investigate the physical processes in the M-I system driving them and their relation to current-inducing events.

Acknowledgments

The tables of TLA events and space weather association information, as well as the algorithm developed for this research are available on the University of Michigan Deep Blue data repository (doi.org/10.7302/9t46-0092).

The authors thank the MACCS team for data (space.augsburg.edu/maccs/requestdatafile.jsp). MACCS is operated by the University of Michigan and Augsburg University and funded by the U.S. National Science Foundation via grants AGS-2013433 and AGS-2013648.

We gratefully acknowledge the SuperMAG collaborators (supermag.jhuapl.edu/info/?page=acknowledgement)

The results presented in this paper rely on the SC Event List calculated and made available by Observatori de L'Ebre, Spain from data collected at magnetic observatories. We thank the involved national institutes, the INTERMAGNET network and ISGI (obsebre.es/en/rapid).

The authors thank Mike Hapgood for his comments as a referee of this research letter.

References

- Amm, O., & Viljanen, A. (1999). Ionospheric disturbance magnetic field continuation from the ground to the ionosphere using spherical elementary current systems. *Earth, Planets and Space*, *51*(6), 431–440. doi: 10.1186/BF03352247
- Belakhovsky, V., Pilipenko, V., Engebretson, M., Sakharov, Y., & Selivanov, V. (2019). Impulsive disturbances of the geomagnetic field as a cause of induced currents of electric power lines. *Journal of Space Weather and Space Climate*, *9*, 1–19. doi: 10.1051/swsc/2019015
- Boteler, D. H., & Beek, G. J. V. (1999). August 4, 1972 revisited: A new look at the geomagnetic disturbance that caused the L4 cable system outage. *Geophysical Research Letters*, *26*(5), 577–580.
- Boteler, D. H., Pirjola, R. J., & Nevanlinna, H. (1998). The effects of geomagnetic disturbances on electrical systems at the Earth’s surface. *Advances in Space Research*, *22*(1), 17–27. doi: 10.1016/S0273-1177(97)01096-X
- Curto, J. J., Araki, T., & Alberca, L. F. (2007). Evolution of the concept of sudden storm commencements and their operative identification. *Earth, Planets and Space*, *59*(11). doi: 10.1186/BF03352059
- Dimmock, A. P., Rosenqvist, L., Welling, D. T., Viljanen, A., Honkonen, I., Boynton, R. J., & Yordanova, E. (2020). On the Regional Variability of dB/dt and Its Significance to GIC. *Space Weather*, *18*(8), 1–20. doi: 10.1029/2020SW002497
- Engebretson, M. J., Pilipenko, V. A., Ahmed, L. Y., Posch, J. L., Steinmetz, E. S., Moldwin, M. B., ... Vorobev, A. V. (2019a). Nighttime Magnetic Perturbation Events Observed in Arctic Canada: 1. Survey and Statistical Analysis. *Journal of Geophysical Research: Space Physics*, *124*(9), 7442–7458. doi: 10.1029/2019JA026794
- Engebretson, M. J., Pilipenko, V. A., Steinmetz, E. S., & Moldwin, M. B. (2021). Nighttime magnetic perturbation events observed in Arctic Canada : 3 . Occurrence and amplitude as functions of magnetic latitude , local time , and magnetic disturbance indices.
- Engebretson, M. J., Steinmetz, E. S., Posch, J. L., Pilipenko, V. A., Moldwin, M. B., Connors, M. G., ... Kistler, L. M. (2019b). Nighttime Magnetic Perturbation Events Observed in Arctic Canada: 2. Multiple-Instrument Observations.

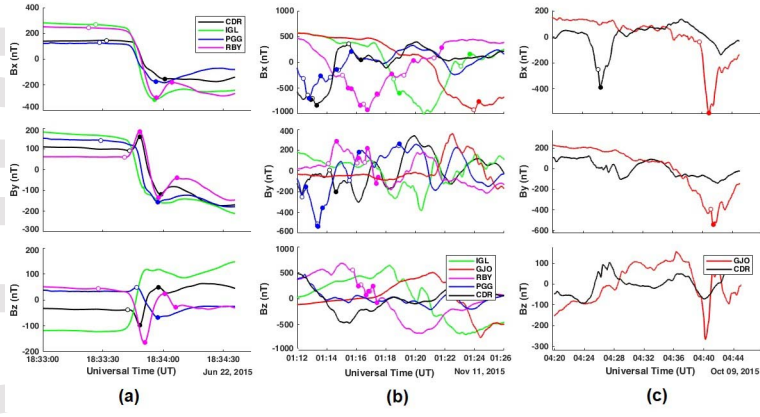
- Journal of Geophysical Research: Space Physics*, 124(9), 7459–7476. doi: 10.1029/2019JA026797
- Gjerloev, J. W. (2012). The SuperMAG data processing technique. *Journal of Geophysical Research: Space Physics*, 117(9), 1–19. doi: 10.1029/2012JA017683
- Hughes, W., & Engebretson, M. (1997). MACCS: Magnetometer array for cusp and cleft studies. *Satellite - Ground Based Coordination Sourcebook. ESA SP-1198*(1), 119.
- Kappenman, J. G. (2005). An overview of the impulsive geomagnetic field disturbances and power grid impacts associated with the violent Sun-Earth connection events of 29-31 October 2003 and a comparative evaluation with other contemporary storms. *Space Weather*, 3(8). doi: 10.1029/2004SW000128
- Kappenman, J. G. (2006). Great geomagnetic storms and extreme impulsive geomagnetic field disturbance events - An analysis of observational evidence including the great storm of May 1921. *Advances in Space Research*, 38(2), 188–199. doi: 10.1016/j.asr.2005.08.055
- Kataoka, R., & Ngwira, C. (2016). Extreme geomagnetically induced currents. , 3(1). Retrieved from <http://dx.doi.org/10.1186/s40645-016-0101-x> doi: 10.1186/s40645-016-0101-x
- Khomutov, S. Y., Mandrikova, O. V., Budilova, E. A., Arora, K., & Manjula, L. (2017). Noise in raw data from magnetic observatories. *Geoscientific Instrumentation, Methods and Data Systems*, 6(2), 329–343. doi: 10.5194/gi-6-329-2017
- Newell, P. T., & Gjerloev, J. W. (2011). Substorm and magnetosphere characteristic scales inferred from the SuperMAG auroral electrojet indices. *Journal of Geophysical Research: Space Physics*, 116(12), 1–15. doi: 10.1029/2011JA016936
- Newell, P. T., & Gjerloev, J. W. (2012). SuperMAG-based partial ring current indices. *Journal of Geophysical Research: Space Physics*, 117(5), 1–15. doi: 10.1029/2012JA017586
- Nguyen, N., Muller, P., & Collin, J. (2020). The Statistical Analysis of Noise in Triaxial Magnetometers and Calibration Procedure. *2019 16th Workshop on Positioning, Navigation and Communications (WPNC)*, 1–6. doi: 10.1109/wpnc47567.2019.8970255
- Ngwira, C. M., Pulkkinen, A., McKinnell, L. A., & Cilliers, P. J. (2008). Improved

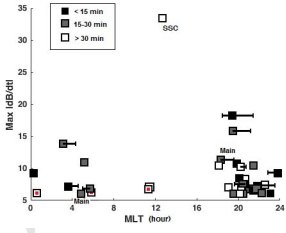
- modeling of geomagnetically induced currents in the South African power network. *Space Weather*, 6(11). doi: 10.1029/2008SW000408
- Ngwira, C. M., Pulkkinen, A. A., Bernabeu, E., Eichner, J., Viljanen, A., & Crowley, G. (2015). Characteristics of extreme geoelectric fields and their possible causes: Localized peak enhancements. *Geophysical Research Letters*, 42(17), 6916–6921. doi: 10.1002/2015GL065061
- Ngwira, C. M., Sibeck, D., Silveira, M. V., Georgiou, M., Weygand, J. M., Nishimura, Y., & Hampton, D. (2018). A Study of Intense Local dB/dt Variations During Two Geomagnetic Storms. *Space Weather*, 16(6), 676–693. doi: 10.1029/2018SW001911
- Opgenoorth, H. J., Schilling, A., & Hamrin, M. (2020). GIC Drivers- Characteristics of Storm-time Rapid Geomagnetic Variations. *EGU General Assembly 2020*, Online, 4-8 May 2020, EGU2020-5667. doi: <https://doi.org/10.5194/egusphere-egu2020-5667>
- Oyedokun, D., Heyns, M., Cilliers, P., & Gaunt, C. T. (2020). Frequency components of geomagnetically induced currents for power system modelling. *2020 International SAUPEC/RobMech/PRASA Conference, SAUPEC/RobMech/PRASA 2020*. doi: 10.1109/SAUPEC/RobMech/PRASA48453.2020.9041021
- Pulkkinen, A., Bernabeu, E., Eichner, J., Viljanen, A., & Ngwira, C. (2015). Regional-scale high-latitude extreme geoelectric fields pertaining to geomagnetically induced currents. *Earth, Planets and Space*, 67(1). Retrieved from <http://dx.doi.org/10.1186/s40623-015-0255-6> doi: 10.1186/s40623-015-0255-6
- Pulkkinen, A., Bernabeu, E., Thomson, A., Viljanen, A., Pirjola, R., Boteler, D., ... MacAlester, M. (2017). Geomagnetically induced currents: Science, engineering, and applications readiness. *Space Weather*, 15(7), 828–856. doi: 10.1002/2016SW001501
- Pulkkinen, A., Viljanen, A., & Pirjola, R. (2006). Estimation of geomagnetically induced current levels from different input data. *Space Weather*, 4(8). doi: 10.1029/2006SW000229
- Simpson, J. J. (2011). On the possibility of high-level transient coronal mass ejection-induced ionospheric current coupling to electric power grids. *Jour-*

nal of Geophysical Research: Space Physics, 116(11), 1–12. doi: 10.1029/2011JA016830

Weygand, J. M., Amm, O., Viljanen, A., Angelopoulos, V., Murr, D., Engebretson, M. J., ... Mann, I. (2011). Application and validation of the spherical elementary currents systems technique for deriving ionospheric equivalent currents with the North American and Greenland ground magnetometer arrays. *Journal of Geophysical Research: Space Physics*, 116(3), 1–8. doi: 10.1029/2010JA016177

Zhang, J. J., Wang, C., & Tang, B. B. (2012). Modeling geomagnetically induced electric field and currents by combining a global MHD model with a local one-dimensional method. *Space Weather*, 10(5), 1–11. doi: 10.1029/2012SW000772





TLA Events

